The significance of the 5′-flanking regions of a gene for transcriptional control has been shown for several other genes. Fusion of the 5′-flanking region of a growth hormone, metallothionein or heat shock gene to the HSV *tk* transcription unit yielded hybrid genes inducible by glucocorticoids[18], cadmium ion[19] or heat[20], respectively. Similarly, the 5′-flanking region of mouse mammary tumour virus DNA rendered a dihydrofolate reductase transcription unit responsive to glucocorticoids[21]. In contrast, Pitha and her colleagues[22,23] concluded that the elements essential for IFN-β induction lie within the coding or 3′ noncoding region; these results require independent confirmation.

Which parts of the 5′-flanking sequence of the IFN-α_1 gene are required for transcription? We have shown that the ATA box is essential for β-globin transcription from the hybrid gene, and that the transcripts initiate 30 ± 3 bp downstream of the ATA box and not at the cap site of the β-globin gene. These results confirm the role generally attributed to the ATA box, namely that of determining the transcription initiation site and sustaining maximal transcription of many (but not all) genes[9,24,25]. In the accompanying paper[26] we have shown that deletions removing all but 117 nucleotides of the 5′-flanking region of the IN-α_1 gene do not abolish inducible transcription. Therefore, a DNA segment extending from position −117 to −6 suffices for inducible transcription. Further insights may be obtained by testing hybrid promoters, composed of elements from the IFN-α and the β-globin 5′-flanking sequence.

This work was supported by the Schweizerissche Nationalfonds (3.147.81), the Deutsche Forschungsgemeinschaft and the Kanton of Zürich. We thank S. Nagarta and A. van Ooyen for plasmids, P. Dierks and J.-I. Fujisawa for [γ-^{32}P]ATP, H. Arnheiter for NDV and N. Mantei for comments on the manuscript.

Received 1 February; accepted 29 March 1983.

1. Stewart, W. II. *The Interferon System* (Springer, New York, 1979).
2. Berg, K. *Acta path. microbiol. immun. scand.* Sect. C, Suppl. 279 (1982).
3. Raj, N. & Pitha, P. *Proc. natn. Acad. Sci. U.S.A.* **78,** 7426–7430 (1981).
4. Cavalieri, R., Havell, E., Vilcek, J. & Pestka, S. *Proc. natn. Acad. Sci. U.S.A.* **74,** 4415–4419 (1977).
5. Sehgal, P., Dobberstein, B. & Tamm, I. *Proc. natn. Acad. Sci. U.S.A.* **74,** 3409–3413 (1977).
6. Morser, J. *et al. J. gen. Virol.* **44,** 231–234 (1979).
7. Mantei, N. & Weissmann, C. *Nature* **297,** 128–132 (1982).
8. Dierks, P., van Ooyen, A., Mantei, N. & Weissmann, C. *Proc. natn. Acad. Sci. U.S.A.* **78,** 1411–1415 (1981).
9. Dierks, P. *et al. Cell* **32,** 695–706 (1983).
10. Berk, A. J. & Sharp, P. A. *Cell* **12,** 721–732 (1977).
11. Weaver, R. & Weissmann, C. *Nucleic Acids Res.* **7,** 1175–1193 (1979).
12. Mantei, N., Boll, W. & Weissmann, C. *Nature* **281,** 40–46 (1979).
13. Grosveld, G., de Bower, E., Shewmaker, C. K. & Flavell, R. A. *Nature* **295,** 120–126 (1982).
14. Shaw, G. D. *et al. Nucleic Acids Res.* **11,** 555–573 (1983).
15. Wilson, D. E. *J. Virol.* **2,** 1–6 (1968).
16. Thacore, H. & Youngner, J. S. *J. Virol.* **6,** 42–48 (1970).
17. Vollock, V. & Housman, D. *Cell* **23,** 509–514 (1981).
18. Robins, D., Peacock, I., Seeburg, P. & Axel, R. *Cell* **29,** 623–631 (1982).
19. Majo, K., Warren, R. & Palmiter, R. *Cell* **29,** 99–108 (1982).
20. Pelham, H. R. B. *Cell* **30,** 517–528 (1982).
21. Lee, F., Mulligan, R., Berg, P. & Ringold, G. *Nature* **294,** 228–232 (1981).
22. Reyes, G. *et al. Nature* **297,** 597–601 (1982).
23. Pitha, P. *et al. Proc. natn. Acad. Sci. U.S.A.* **79,** 4337–4341 (1982).
24. Grosschedl, R. & Birnstiel, M. L. *Proc. natn. Acad. Sci. U.S.A.* **77,** 1432–1436 (1980).
25. Benoist, C. & Chambon, P. *Nature* **290,** 304–310 (1981).
26. Ragg, H. & Weissmann, C. *Nature* **303,** 439–442 (1983).
27. Nagata, S., Mantei, N. & Weissmann, C. *Nature* **287,** 401–408 (1980).
28. Chalberg, M. & Englund, P. *Meth. Enzym.* **65,** 39–43 (1980).
29. van Ooyen, A., van den Berg, J., Mantei, N. & Weissmann, C. *Science* **206,** 337–344 (1979).
30. Grunstein, D. & Hogness, D. *Proc. natn. Acad. Sci. U.S.A.* **72,** 3961–3965 (1975).
31. Maxam, A. & Gilbert, W. *Proc. natn. Acad. Sci. U.S.A.* **74,** 560–564 (1977).
32. Wilkie, N. *et al. Nucleic Acids Res.* **7,** 859–877 (1979).
33. Aviv, H. & Leder, P. *Proc. natn. Acad. Sci. U.S.A.* **69,** 1408–1412 (1972).
34. Bernardi, G. *Meth. Enzym.* **21,** 95–147 (1971).

Polyoma virus 'hexamer' tubes consist of paired pentamers

Timothy S. Baker*, Donald L. D. Caspar* & William T. Murakami†

* Rosenstiel Basic Medical Sciences Research Center and †Department of Biochemistry, Brandeis University, Waltham, Massachusetts 02254, USA

The discovery that the 72 capsomeres of the icosahedrally symmetric polyoma virus capsid are all pentamers[1] shows that the expected quasi-equivalent bonding specificity[2] is not conserved in the assembly of this virus coat protein. Tubular particles produced by polyoma and other papovaviruses seem to be polymorphic aggregates of capsomeres[3] that may arise through variation in switching of the bonding specificity. Electron micrographs of wide and narrow classes of tubes were analysed by Kiselev and Klug[4] using optical diffraction and optical filtering methods. The wide type were called 'hexamer' tubes because they consist of approximately hexagonally arrayed capsomeres that were assumed to be hexamers[4], in accord with the quasi-equivalence theory of icosahedral virus particle construction[2]. The narrow type were called 'pentamer' tubes because the capsomeres are arrayed in a particular 'pentagonal tessellation' which arises from the pairing of pentamers across 2-fold axes of the surface lattice[4]. Our reexamination of negatively-stained polyoma virus tubes by digital image processing of low-irradiation electron micrographs shows that all tubes are assemblies of paired pentameric capsomeres. We report here that the packing arrangement of the pentamers in the hexamer tubes is simply related to the pentagonal tessellation[4] representing the packing in the narrow pentamer tubes. In all the tube structures examined, at least one pairwise contact between neighbouring pentamers closely resembles the contact between the pentavalent and hexavalent capsomeres in the icosahedral capsid[1].

Specimens were prepared from polyoma virus fractions sedimenting between the virion and capsid peaks on a sucrose density gradient. Electron micrographs of the negatively-stained specimens show the order of one tubular particle for every 100 icosahedral particles (diameter 450–500 Å). The most frequent tube structures (Fig. 1*A*) have a diameter of 400–450 Å and are built of approximately hexagonally packed capsomeres arrayed with one of the lattice lines at a small angle to the particle axis. Similar hexagonal packing is observed in tubes of diameter ranging from 275 to 525 Å. Micrographs of shadowed specimens show that the tubes are flattened and the near axial rows of capsomeres are inclined to the left, thus defining the hand of the surface lattices. About 10% of the tubes are the narrow (~300 Å diameter) pentamer type[4].

Diffraction patterns were computed from images of minimally irradiated ($< 20\ e^- Å^{-2}$) specimens[5], negatively stained with 1% uranyl acetate. Figure 1*B* is representative of the hexamer tube diffraction patterns. The patterns from the front and back sides are related by approximate mirror symmetry about the meridional axis. Twelve pairs of dominant spots due to diffraction from the top hexagonal array of capsomeres (away from the grid as established from shadowed specimens) are marked by circles in Fig. 1*C*. This indexing, which is the same as that defined by Kiselev and Klug[4], omits six additional spots, marked by squares, located at positions corresponding to a repeating unit of twice the area of the simple hexagonal unit cell. The intensity of these additional spots is sensitive to irradiation, although some are still evident even after exposure to $> 100\ e^- Å^{-2}$. For example, in the first analysed diffraction pattern from a polyoma virus hexamer tube[4] (from a micrograph recorded with conventional high irradiation) one strong and several weak spots from the larger unit cell can be discerned, as we now know where to look. Our scheme for indexing the hexamer tube diffraction pattern identifies a near orthogonal unit cell. From the average of measurements on 18 flattened hexamer tubes, the cell dimensions for the front surface are 89×137 Å subtending an angle of 83° and the cell is oriented with the short axis at ~45° to the right of the tube axis; for

0028–0836/83/220446—03$01.00

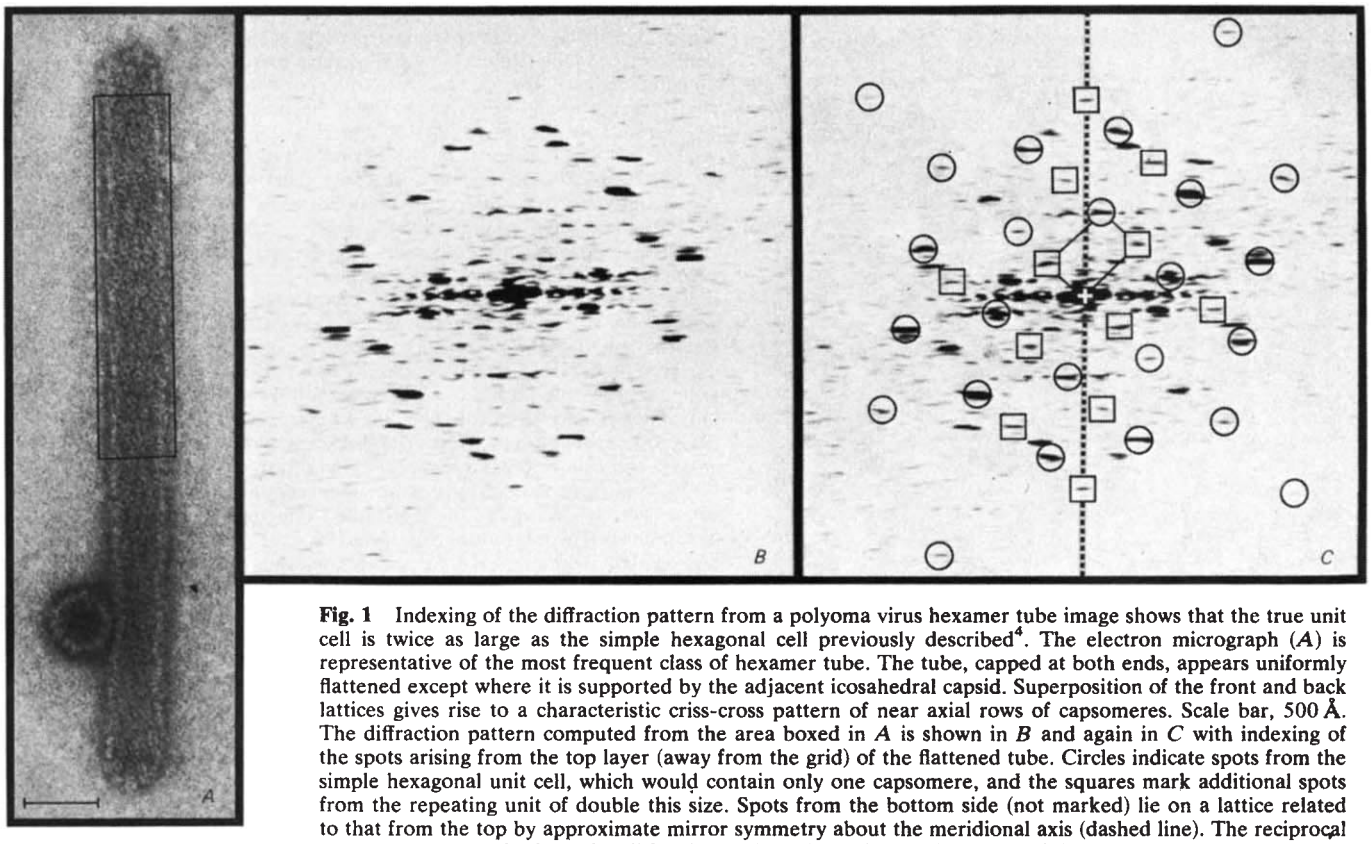

Fig. 1 Indexing of the diffraction pattern from a polyoma virus hexamer tube image shows that the true unit cell is twice as large as the simple hexagonal cell previously described[4]. The electron micrograph (*A*) is representative of the most frequent class of hexamer tube. The tube, capped at both ends, appears uniformly flattened except where it is supported by the adjacent icosahedral capsid. Superposition of the front and back lattices gives rise to a characteristic criss-cross pattern of near axial rows of capsomeres. Scale bar, 500 Å. The diffraction pattern computed from the area boxed in *A* is shown in *B* and again in *C* with indexing of the spots arising from the top layer (away from the grid) of the flattened tube. Circles indicate spots from the simple hexagonal unit cell, which would contain only one capsomere, and the squares mark additional spots from the repeating unit of double this size. Spots from the bottom side (not marked) lie on a lattice related to that from the top by approximate mirror symmetry about the meridional axis (dashed line). The reciprocal lattice unit cell for the top layer is marked at the centre of the pattern.

the back surface (in contact with the support film) the dimensions of the approximately mirror symmetric cell are 95×147 Å, subtending an angle of 89°. The shrinkage of the top surface relative to the bottom is typical for negatively-stained specimens[6].

The filtered image (Fig. 2*A*), computed for the front layer using the 18 pairs of spots indexed in Fig. 1*C*, shows the packing arrangement of the pair of capsomeres in the unit cell. The capsomeres appear pentagonally shaped in the clearest parts of the filtered image and are arranged in a surface lattice having p2 symmetry. Models built of regularly packed, pentagonally symmetric units have been constructed to fit the features seen in the filtered micrographs. A computer-generated image of the front view of the planar model (with lattice dimension corresponding to the upper layer of the flattened tube) is compared with the filtered electron micrograph in Fig. 2*B*.

The relation of the pentamer packing in the hexamer tubes to that in the pentamer tubes[4] is illustrated in Fig. 3. Common to both is a zigzag ribbon arrangement of pentamers connected by adjacent edge-to-edge contacts; this ribbon motif is inclined at an angle of ~45° up to the right of the tube axis. Within a ribbon in the tube surface, the adjacent edge-to-edge dimer contacts are of two different types: one indicated by the nearly vertical 'zig' lines in Fig. 3 between the pentamer pairs oriented in the axial direction, and the other by the nearly horizontal 'zag' lines between the pentamer pairs in the direction of maximum curvature. Each pentamer in the zigzag ribbons of the pentamer tube tessellation[4] (Fig. 3*B*) makes a third type of edge-to-edge dimer contact in a diagonal direction (inclined up to the left) with a pentamer in a neighbouring ribbon. In the hexamer tube surface lattice (Fig. 3*A*), the ribbons are shifted so that each pentamer makes a short edge-overlap dimer contact and a vertex-to-vertex pairing with two pentamers in an adjacent ribbon. The directions of these two types of inter-ribbon contacts in the hexamer tube lattice are nearly parallel to the zig and zag lines in Fig. 3*A*. This hexagonally coordinated arrangement of pentamers produces a pattern of unequally spaced pairs of small triangular gaps

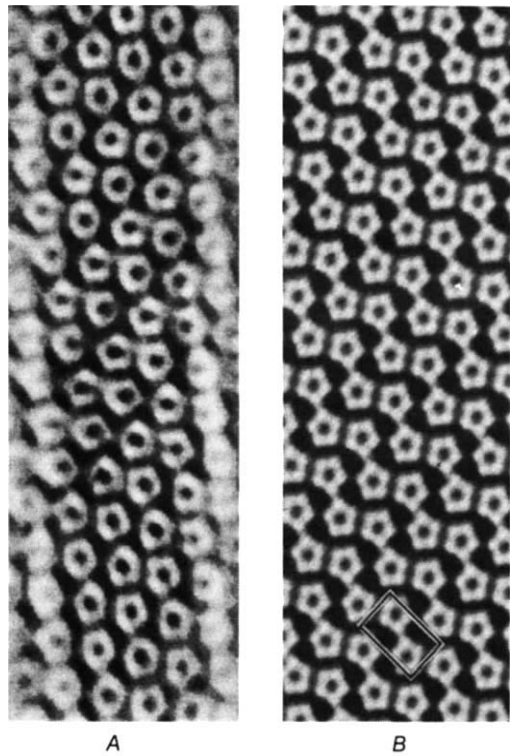

Fig. 2 The filtered image of the front layer of a flattened hexamer tube corresponds to a model surface lattice built of pairs of pentamers arrayed with p2 symmetry. Image *A* was computed from the diffraction pattern of the portion of the tube boxed in Fig. 1*A*. The pattern was filtered to include the spots indexed in Fig. 1*C* and the equator (with the equator and the meridional pair of spots given half weighting). The planar model (*B*) was built in the computer from regular pentamers arranged in a p2 lattice at the coordinates measured for the capsomeres in the unit cell of the filtered image. One choice of unit cell is boxed.

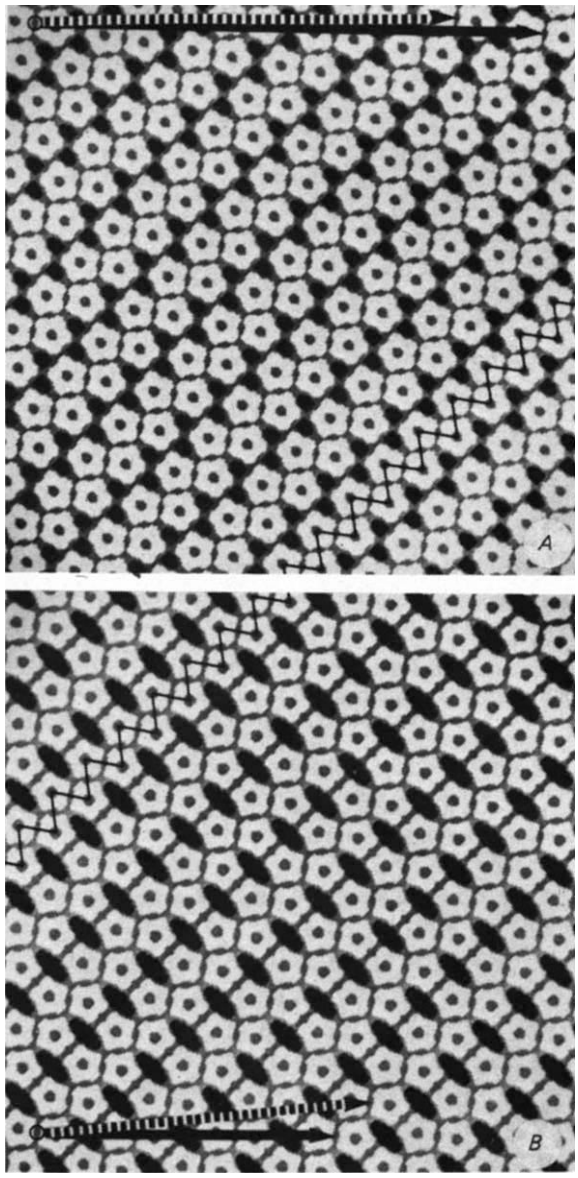

Fig. 3 Comparison of the pentamer packing in hexamer (*A*) and pentamer (*B*) tube surface lattices illustrates correspondences in bonding contacts. The 'zig' and 'zag' lines (oriented respectively nearly vertically and horizontally along the diagonally directed ribbon) indicate the two classes of dimer 'bonds' between pentamers that are conserved in the hexamer and pentamer tube lattices. These planar models were constructed with equivalent connections for the differently oriented edge-to-edge bonds between the pentagonal units, and the packing width of the zigzag ribbon in *A* was made the same as in *B*. In the cylindrically curved tube surface, the differently oriented edge-to-edge contacts are non-equivalently bent. Furthermore, the relative separations of capsomeres in the different bonding directions measured from electron micrographs are slightly distorted compared to these idealized models. Circumferential vectors corresponding to different tube structures are marked by arrows between equivalent lattice points. Models of the tubes can be constructed from these plane lattices by cutting out rectangles based on the circumferential vectors and connecting the vertical edges to form cylinders. Two of the frequently observed size of hexamer tubes are indicated by the arrows at the top of *A*, the dashed one representing the circumference of the tube in Fig. 1*A*. Hexamer tubes of larger and smaller diameter have circumferential vectors in approximately the same direction as the marked arrows. The circumferential vectors of the zero- and one-start pentamer tubes[4] (which are the only identified narrow tubes of this type) are marked by the solid and dashed arrows, respectively, at the bottom of *B*.

between ribbons. Alignment of the ribbons in the pentamer tube lattice to form the diagonal edge-to-edge contacts (Fig. 3*B*) generates the distinctive pattern of large lozenge-shaped gaps that is a dominant feature of the electron microscope images[4].

All the polymorphic tubular assemblies of polyoma virus capsomeres that we have analysed are constructed from paired pentamers. A rare class of wide tube, to be described elsewhere, is built of edge-to-edge bonded pentamer dimers oriented alternately parallel and perpendicular to the tube axis in an approximately square surface lattice. The curvature of all the tubular surface lattices requires bending at the edge-to-edge connection between the pentamer pairs oriented in the circumferential direction. We infer that this bent contact between pentamers in the wide hexamer tubes is similar to the edge-to-edge connection between the pentavalent and hexavalent pentamers in the capsid[1], whose axes subtend an angle of ~25°; greater bending of the circumferentially oriented pentamer pairs is needed to form the narrow pentamer tubes. The two other types of contacts identified between pairs of hexavalent pentamers in the capsid[1] are similar to the two kinds of dimer contacts between pentamers of adjacent zigzag ribbons in the hexamer tubes. Thus, the polymorphism of the tubular aggregates correlates with the variable bonding potential of the pentameric capsomeres evident in the icosahedral capsid.

The quasi-equivalence theory of icosahedral virus particle construction[2] required hexamers as well as pentamers of the protein subunits to conserve bonding specificity. Previous observations on the structure of papovavirus capsids and their polymorphic variants were believed to be consistent with this theory. In retrospect, there was no compelling experimental evidence to support the belief in the existence of hexameric capsomeres in papovaviruses. Our recent X-ray diffraction[1,7,8] and electron microscopy studies are compatible with the previous observations and show that all polyoma virus capsomeres are in fact pentamers. The logic of the all-pentamer assembly may be explained by a capsomere model with switchable bonding specificity that can build the icosahedral capsid and the polymorphic tubes.

We thank Drs I. Rayment and D. DeRosier for discussions and suggestions, and P. Flicker for help with the shadowing experiments. This project was supported in part by USPHS grant CA15468 from the NCI to D.L.D.C. and Biomedical Research Support Grant RR07044.

Received 10 February; accepted 7 April 1983.

1. Rayment, I., Baker, T. S., Caspar, D. L. D. & Murakami, W. T. *Nature* **295**, 110–115 (1982).
2. Caspar, D. L. D. & Klug, A. *Cold Spring Harb. Symp. quant. Biol.* **27**, 1–24 (1962).
3. Finch, J. T. & Klug, A. *J. molec. Biol.* **13**, 1–12 (1965).
4. Kiselev, N. A. & Klug, A. *J. molec. Biol.* **40**, 155–171 (1969).
5. Baker, T. S. & Amos, L. A. *J. molec. Biol.* **123**, 89–106 (1978).
6. Moody, M. F. *J. molec. Biol.* **25**, 167–200 (1967).
7. Rayment, I. *Acta crystallogr.* **A39**, 102–116 (1983).
8. Rayment, I., Baker, T. S. & Caspar, D. L. D. *Acta crystallogr.* **B39** (1983).